JOURNAL OF AGRICULTURAL AND FOOD CHEMISTRY

pubs.acs.org/JAFC

Article

# Engineering of Multiple Modules to Improve Amorphadiene Production in *Bacillus subtilis* Using CRISPR-Cas9

Yafeng Song, Siqi He, Ingy I. Abdallah, Anita Jopkiewicz, Rita Setroikromo, Ronald van Merkerk, Pieter G. Tepper, and Wim J. Quax*

Cite This: *J. Agric. Food Chem.* 2021, 69, 4785−4794

Read Online

ACCESS | Metrics & More | Article Recommendations | Supporting Information

**ABSTRACT:** Engineering strategies to improve terpenoids' production in *Bacillus subtilis* mainly focus on 2*C*-methyl-D-erythritol-4-phosphate (MEP) pathway overexpression. To systematically engineer the chassis strain for higher amorphadiene (precursor of artemisinin) production, a clustered regularly interspaced short palindromic repeat-Cas9 (CRISPR-Cas9) system was established in *B. subtilis* to facilitate precise and efficient genome editing. Then, this system was employed to engineer three more modules to improve amorphadiene production, including the terpene synthase module, the branch pathway module, and the central metabolic pathway module. Finally, our combination of all of the useful strategies within one strain significantly increased extracellular amorphadiene production from 81 to 116 mg/L after 48 h flask fermentation without medium optimization. For the first time, we attenuated the FPP-derived competing pathway to improve amorphadiene biosynthesis and investigated how the TCA cycle affects amorphadiene production in *B. subtilis*. Overall, this study provides a universal strategy for further increasing terpenoids' production in *B. subtilis* by comprehensive and systematic metabolic engineering.

**KEYWORDS:** *Bacillus subtilis, CRISPR-Cas9, MEP, amorphadiene synthase, TCA cycle, metabolic engineering*

## INTRODUCTION

Terpenoids, also known as isoprenoids, are a large group of natural products that are extensively used in food, cosmetic, pharmaceutical, and agricultural industries due to their versatile bioactivities.[1,2] Chemically, they are divided into different categories according to the number of basic five-carbon isoprene units in their skeletons, including hemiterpenoids ($C_5$), monoterpenoids ($C_{10}$), sesquiterpenoids ($C_{15}$), diterpenoids ($C_{20}$), triterpenoids ($C_{30}$), and polyterpenoids ($C_{>30}$). As secondary metabolites in plants, the yield of many terpenoids is extremely low and their structural complexities make chemical synthesis difficult.[3] With the rapidly increasing demands for terpenoids, microbial cells have garnered vast attention as hosts for the production of valuable natural products.[4−7] Generally regarded as safe, *Bacillus subtilis* has recently demonstrated its high potential as a bacterial platform for terpenoids' production. It possesses the endogenous 2*C*-methyl-D-erythritol-4-phosphate (MEP) pathway to produce the terpene precursor isopentenyl pyrophosphate (IPP) and its isomer dimethylallyl pyrophosphate (DMAPP) (Figure 1). By introducing relevant terpene synthases and metabolic engineering optimization, *B. subtilis* is able to produce multiple terpenoids, with the production levels ranging from 1.43 to 416 mg/L.[8−19]

However, most of the strategies to improve terpenoids' production rely on the overexpression of rate-limiting or all enzymes of the MEP pathway, selection of suitable expression vectors for terpene synthases, and optimization of fermentation conditions such as cultivation temperature and medium.[8,9,16] Very little work has been done to explore the effects of other related pathways on terpenoids' production. For example, the competing branch pathways can limit the availability of IPP and DMAPP, and the central metabolic pathways might directly or indirectly impact the supply of cofactors required by the MEP pathway. Those strategies have not been thoroughly investigated, particularly in *B. subtilis*. The latter approach has been well examined and achieved a 64% increase of the $\beta$-carotene yield in *Escherichia coli*.[20] In that study, key enzymes from three modules including the TCA cycle, pentose phosphate pathway, and ATP synthesis were fine-tuned by editing the inherent promoters at the genomic level. The highest terpenoids' increments were reached by engineering the expression level of TCA enzymes.

Moreover, the systematic methods including genome-wide stoichiometric analysis, transcriptomics, proteomics, and metabolomics allow a global overview of the current status of the genome, transcripts, proteins, and metabolism within the bacteria, providing us with plenty of promising targets to explore.[21−26] All of these indicated the importance of comprehensively engineering the different modules involved in the terpenoid biosynthesis pathway.[17,20] To explore whether this strategy also facilitates the improvement of terpenoids' production in *B. subtilis*, increasing the production of amorphadiene, the important precursor of the antimalarial drug artemisinin, was selected for investigation. At least four modules could be the engineering targets, including the

Received: January 25, 2021
Revised: April 6, 2021
Accepted: April 8, 2021
Published: April 20, 2021





https://doi.org/10.1021/acs.jafc.1c00498
*J. Agric. Food Chem.* 2021, 69, 4785−4794

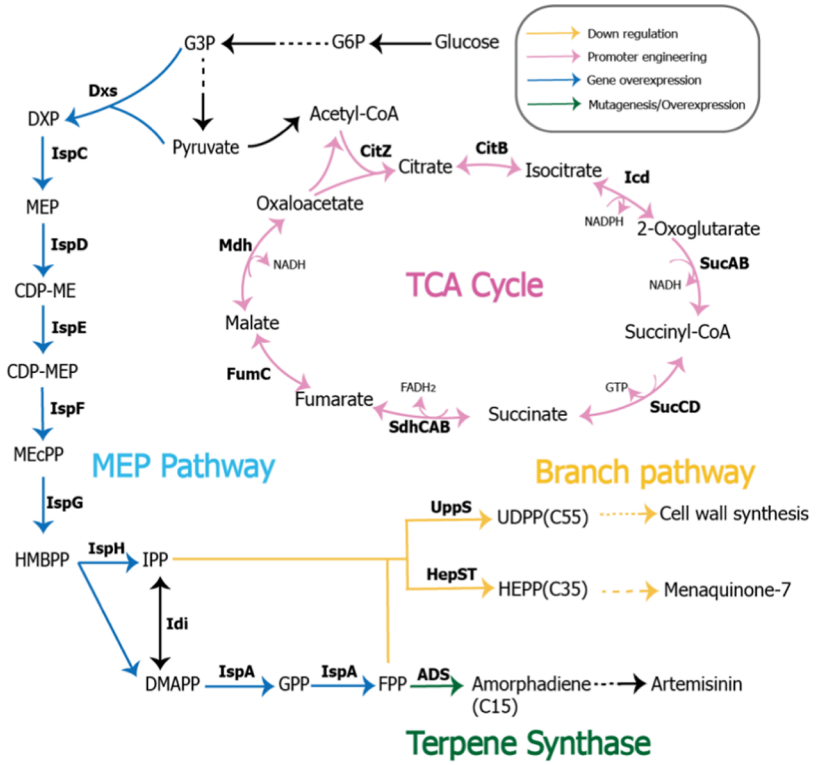


**Figure 1.** Engineering strategies to improve amorphadiene production in *B. subtilis*. Four modules were engineered, including increasing MEP pathway gene expression, decreasing competing pathway gene expression, engineering of terpene synthase, and regulation of TCA cycle metabolism by employing either weak or strong promoters. Dxs, 1-deoxy-D-xylulose-5-phosphate synthase; IspC, 1-deoxy-D-xylulose-5-phosphate reductoisomerase; IspD, 4-pyrophosphocytidyl-2-*C*-methyl-D-erythritol synthase; IspE, 4-pyrophosphocytidyl-2-*C*-methyl-D-erythritol kinase; IspF, 2*C*-methyl-D-erythritol 2,4-cyclopyrophosphate synthase; IspG, 1-hydroxy-2-methyl-2-(*E*)-butenyl 4-pyrophosphate synthase; IspH, 1-hydroxy-2-methyl-butenyl 4-pyrophosphate reductase; Idi, isopentenyl pyrophosphate isomerase; IspA, farnesyl pyrophosphate synthase; CitZ, citrate synthase II; CitB, aconitase; Icd, isocitrate dehydrogenase; SucA, 2-oxoglutarate dehydrogenase (E1 subunit); SucB, 2-oxoglutarate dehydrogenase complex (dihydrolipoamide transsuccinylase, E2 subunit); SucC, succinyl-CoA synthetase ($\beta$ subunit); SucD, succinyl-CoA synthetase ($\alpha$ subunit); SdhA, succinate dehydrogenase (flavoprotein subunit); SdhB, succinate dehydrogenase; SdhC, succinate dehydrogenase (cytochrome b558 subunit); FumC, fumarase; Mdh, malate dehydrogenase.Metabolite abbreviations: G3P, glyceraldehyde-3-phosphate; DXP, 1-deoxy-D-xylulose 5-phosphate; MEP, 2-*C*-methyl-D-erythritol 4-phosphate; CDP-ME, 4-(cytidine 5′-pyrophospho)-2-*C*-methyl-D-erythritol; CDP-MEP, 2-phospho-4-(cytidine 5′-pyrophospho)-2-*C*-methyl-D-erythritol; MEcPP, 2-*C*-methyl-D-erythritol 2,4-cyclopyrophosphate; HMBPP; 1-hydroxy-2-methyl-2-butenyl 4-pyrophosphate; IPP, isopentenyl pyrophosphate; DMAPP, dimethylallyl pyrophosphate; GPP, geranyl pyrophosphate; FPP, farnesyl pyrophosphate; HEPP, heptaprenyl diphosphate; UDPP, undecaprenyl pyrophosphate.

amorphadiene synthesis module, branch pathway module, MEP pathway module, and TCA metabolism module.

As is known, efficient and advanced genetic tools accelerate the comprehensive analysis of how different metabolic pathways influence the target product formation, preferably without leaving fragment scars at the genome of the microbial hosts. In *B. subtilis*, most previous scarless genetic tools are based on selection−counterselection techniques, which are time-consuming and have low efficiency due to a limited number of counterselection markers, the toxicity of some compounds required for the selection and/or modified chassis strains with specific mutations.[27] These drawbacks have impeded the accurate and large-scale modification of the *B. subtilis* genome. Currently, the clustered regularly interspaced short palindromic repeats and Cas (CRISPR-Cas9) system is one of the most widely developed genetic engineering tools to perform chromosome modification in eukaryotes and prokaryotes.[28] In *B. subtilis*, this system is also able to overcome the disadvantages mentioned above, is easy to handle, and displays high editing efficiency.

In this study, the CRISPR-Cas9 editing system was first established in a one-plasmid construct and we confirmed its effectiveness in *B. subtilis* for the purpose of further genomic engineering to improve amorphadiene production (Figure 1). Then, desired mutations were introduced into a chromosomally integrated copy of amorphadiene synthase (ADS), aiming at improving ADS catalytic efficiency. Subsequently, the hypothesis of reducing the activity of branch pathways to improve amorphadiene production was explored. Also, for the first time in *B. subtilis*, the expression levels of TCA enzymes were regulated to investigate the influence of the central metabolic pathway on terpenoids' production. Finally, these strategies were combined, aiming at achieving further improvement of amorphadiene production.

## MATERIALS AND METHODS

**Strains and Culture Conditions.** The plasmids and strains used in this study are listed in Tables S1 and S2. To prepare the seed culture of *B. subtilis*, single colonies were selected and incubated at 37 °C overnight. Then, the overnight seed culture was inoculated into 1 mL of 2SR medium (5% yeast extract, 3% tryptone, and 0.3% $K_2HPO_4$) in a 14 mL round-bottom tube with a ratio of 1:100 (v/v) for fermentation, in triplicates per strain. After around 3 h of cultivation, the expression of GFPADS fusion protein or MEP pathway enzymes was induced by adding IPTG to a final concentration of 1 mM and D-xylose at a final


https://doi.org/10.1021/acs.jafc.1c00498
J. Agric. Food Chem. 2021, 69, 4785−4794

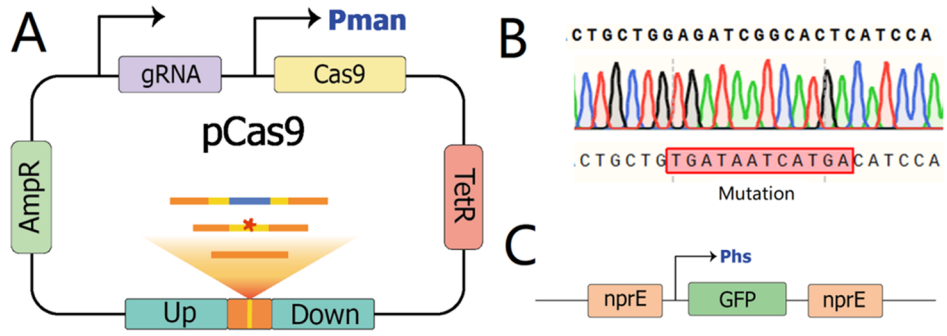


**Figure 2.** CRISPR-Cas9 system in *B. subtilis*. (A) Plasmid scheme of the CRISPR-Cas9 editing plasmid pHY-cas9. $P_{man}$, mannose-inducible promoter $P_{man}$. (B) Mutation of *ugtP* sequence in *B. subtilis*. (C) GFP was integrated into the genome of *B. subtilis* at the *nprE* locus. Phs: promoter $P_{hyperspank}$.

concentration of 1% (m/v) when necessary. The bacterial cultures were then fermented at 20 °C (unless indicated), 230 rpm. Then, bacterial cells and amorphadiene were harvested after a total of 24 h fermentation unless indicated. Antibiotics were added when appropriate (ampicillin at 100 μg/mL for *E. coli*; tetracycline at 15 μg/mL, spectinomycin at 100 μg/mL, and chloramphenicol at 5 μg/mL for *B. subtilis*).

**Plasmid Construction and Transformation.** The prolonged overlap extension polymerase chain reaction (POE-PCR) method was employed to construct the plasmids, as previously described.[29] The SpCas9 coding fragment was amplified from pAW016 and inserted into pHY300PLK under the mannose-inducible promoter $P_{man}$, which was amplified from *B. subtilis* genomic DNA.[30] Subsequently, the gRNA cassette, which targets *ugtP*, was amplified from pAW014-2 and the N20 sequences were replaced by corresponding N20 sequences of target genes. The https://www.benchling.com/crispr/ online tool was used to predict the most suitable PAM and N20 sequences. Moreover, around 1000 bp fragments upstream and downstream the targeting sites were amplified as the editing template (donor DNA) and fused with promoter $P_{hpaII}$ or $P_{liaG}$ in the middle by overlap PCR reactions. The plasmid pP43X and the genome of *B. subtilis* served as the templates for promoter $P_{hpaII}$ and $P_{liaG}$, respectively. Plasmids were constructed using Turbo Competent *E. coli* as the cloning host and were further confirmed by sequencing.

The well-established plasmids (1−2 μg) were then transformed to *B. subtilis* according to standard methods described by Kunst and Rapoport.[31] However, for the CRISPR-Cas9-induced genome editing transformation, a 3 h prolonged incubation before plating the transformation mixture onto the agar plates was performed, aiming at improving the editing efficiency as described by Westbrook et al. (Figure S1).[30] To confirm whether the desired mutations, insertions, or deletions have been introduced into the genome of *B. subtilis*, colony PCR was conducted to amplify the target fragments from the bacterial genome and validated by further sequencing (Figure S2).

**Sample Preparation for Gas Chromatography Detection and Quantification.** The samples were prepared according to the previously published method.[8] Briefly, a 15% (v/v) dodecane (Sigma-Aldrich, Zwijndrecht, The Netherlands) layer containing 56 mg/L β-caryophyllene as the internal standard was added after induction of the bacterial cultures, thus trapping the produced amorphadiene. After 24 h of incubation, the dodecane layers were collected and diluted to amorphadiene concentrations ranging from 3.5 to 28 mg/L. Sample analysis was performed on a Shimadzu GCMS-QP2010Plus system equipped with a GC-2010 Plus gas chromatograph (GC) and an AOC-20i autoinjector. Amorphadiene-containing extracts (2 μL) were injected splitless into the HP-5MS (5% phenyl)-methylpolysiloxane GC column (Agilent J&W 0.25 mm inner diameter, 0.25 μm thickness, 30 m length). The injector temperature was set at 250 °C, and the column oven initial temperature was started at 100 °C for 3 min, with an increase of 15 °C/min to 130 °C and then 5 °C/min until 180 °C, followed by a temperature increase to 280 °C at a rate of 20 °C/min and finally held for 10 min. To monitor $m/z$ ion 189, the MS detector was set to selected ion mode (SIM). The β-caryophyllene (Extrasynthese, Lyon, France) standard curve was used to calculate the concentration of amorphadiene, which was represented as the β-caryophyllene equivalent.

## RESULTS

**Establishing the CRISPR-Cas9 System in *B. subtilis*.** To construct the CRISPR-Cas9 editing vector, we chose one of the smallest hybrid chimeric shuttle plasmids, pHY300PLK, as the backbone to carry SpCas9, the gRNA cassette, and the engineered homologous editing template (Figure 2A). Compared to theta-replicating plasmids, the segregation instability of this rolling circle plasmid gives it a priority to evict plasmids under antibiotic-free conditions after editing events are accomplished, which will facilitate iterative genome engineering. SpCas9 is controlled by *B. subtilis* mannose-inducible promoter $P_{man}$, in spite of the fact that constitutive expression of SpCas9 has been reported to be nontoxic to *B. subtilis*.[30] $P_{man}$ displays activity only when mannose is provided and glucose is absent in *B. subtilis*, but it is absolutely inactive in *E. coli*.[32] The corresponding gRNA cassette is controlled by $P_{xlyA.sphI+1}$, which enables gRNA transcription.[30] This promoter was originated from *B. subtilis*, and the sequence of this promoter was "5′-CATAAAAAACTAAAAAAAATA**TTGAAA**ATACT-GACGAGGTTATA**TAAGAT**GCATGC-3′". The −35, −10, and +1 regions are in bold, and the *Sph*I restriction site is underlined. Editing templates consist of the homology sequences (around 1000 bps for each upstream and downstream arm) flanking the targeting sites and the desired mutations, deletions, or insertions. They are either provided as PCR products or inserted into the editing plasmids. Since the latter form exhibited higher editing efficiency due to the high transformation efficiency, it was applied in our study. As a proof of concept, we successfully introduced mutations into *ugtP* (encoding UDP-glucose diacylglyceroltransferase) using the previously reported gRNA cassette and editing template sequences, to guarantee the functionality of this system in *B. subtilis* (Figure 2B). Moreover, green fluorescent protein (GFP) was successfully integrated into the genome of *B. subtilis* at the *nprE* locus, with editing efficiency higher than 90% (Figures 2C and S2). Thus, we employed this system to conduct further genome engineering investigations to improve the amorphadiene production in *B. subtilis*.

**Engineering of ADS to Improve the Terpenoid, Amorphadiene, Production.** Previously, *gfp* was fused at the N-terminus of *ads* to improve the expression of ADS as a highly expressed fusion protein partner by well adapting to the translation machinery of *B. subtilis*.[8] Then, the fusion *gfpads* followed by the farnesyl pyrophosphate gene (*fpps*) was controlled by IPTG-inducible promoter $P_{hyperspank}$ (Figure 3A).


https://doi.org/10.1021/acs.jafc.1c00498
J. Agric. Food Chem. 2021, 69, 4785−4794

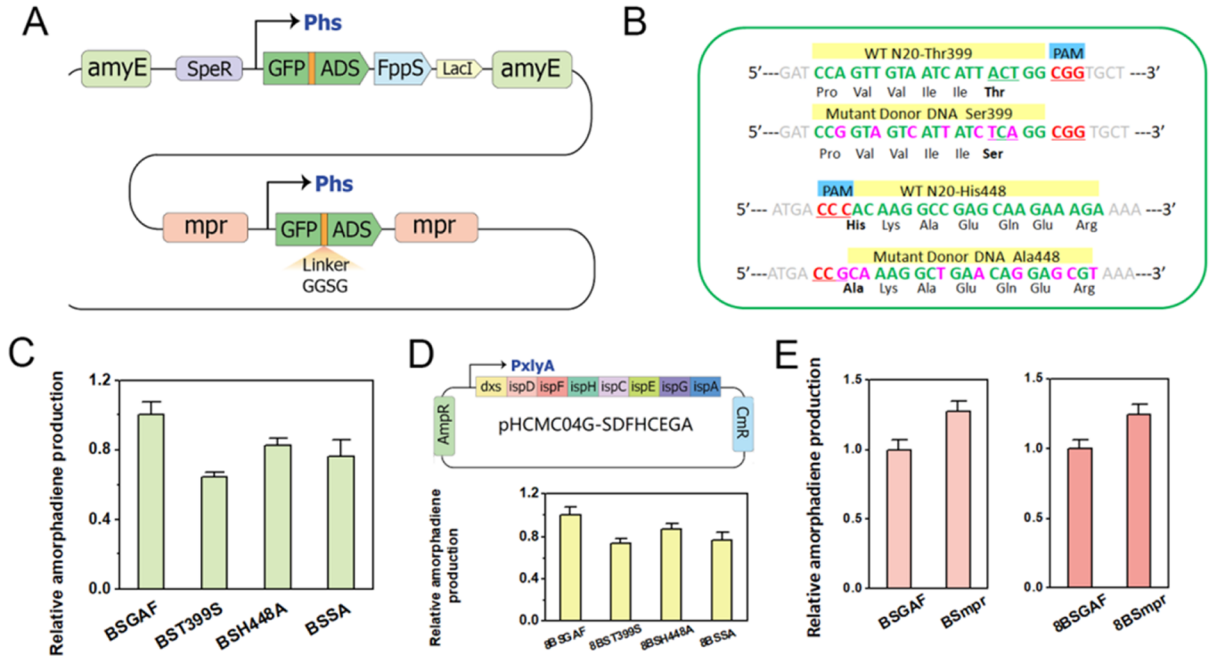


**Figure 3.** Engineering of the genome-integrated amorphadiene synthase (ADS) in *B. subtilis*. (A) ADS was fused with GFP at the N-terminus with a linker GGSG in between. The fusion GFPADS and FppS (farnesyl pyrophosphate synthase) formed an operon under the IPTG-inducible promoter $P_{hyperspank}$ and was integrated into the genome of *B. subtilis* at the *amyE* locus through integrative plasmid pDR111. The second copy of the fusion protein GFPADS was integrated into the *mpr* locus. Phs: promoter $P_{hyperspank}$. (B) Wild-type and mutation sequences of ADS. (C) Relative amorphadiene production by *B. subtilis* strains with different ADS mutations. (D) Plasmid scheme of pHCMC04G-SDFHCEGA, which contains the whole MEP pathway enzymes (encoded by *dxs, ispD, ispF, ispH, ispC, ispE, ispG*) and farnesyl pyrophosphate synthase (*ispA*). Relative amorphadiene production by *B. subtilis* strains with ADS mutations and MEP pathway overexpression. PxylA: Promoter $P_{xylA}$. (E) Relative amorphadiene production by *B. subtilis* strains with an extra copy of GFPADS at the genome, without and with MEP pathway overexpression, after 24 h fermentation. The levels of amorphadiene production of BSGAF and 8BSGAF strains without and with MEP pathway overexpression served as the controls, respectively.

The entire operon was integrated into the genome of *B. subtilis* at the *amyE* locus through integrative plasmid pDR111-GAF, generating strain BSGAF. After 24 h fermentation at 37, 25, and 20 °C, the highest titer of amorphadiene (approximately 13.4 mg/L *β*-caryophyllene equivalent) was obtained when strains were cultured at 20 °C (Figure S3). However, a very limited amount of amorphadiene was detected when strains were incubated at 37 °C, though the fluorescence of GFP displayed similar levels regardless of the temperature. This implied that expression of GFP could not guarantee the correct folding and functionality of ADS. Therefore, it is not feasible to estimate possible amorphadiene levels by measuring fluorescence instead of measuring the concentration of produced amorphadiene through gas chromatography-mass spectrometry (GC-MS), and high ADS activity could not necessarily lead to high amorphadiene productions.

Both previously reported *in vitro* enzymatic studies and *in vivo* ADS expression studies in *E. coli* demonstrated the enhanced catalytic activity of ADS variants T399S, H448A, and double mutant T399S/H448A.[33,34] To explore whether these mutants retain the advantage of improved catalytic activity even in the fused GFPADS form to produce amorphadiene in *B. subtilis*, they were introduced into the genome-integrated GFPADS (BSGAF) by the CRISPR-Cas9 system, generating strains BST399S, BSH448A, and BSSA (Figure 3B). After 24 h fermentation, the amorphadiene produced by GFPADS wild type and mutants was collected and measured. Unfortunately, neither the single nor double mutants produced a higher level of amorphadiene, with T399S, H448A, and T399S/H448A producing only 64, 82, and 76% of amorphadiene compared to wild-type GFPADS (Figures 3C and S4). Subsequently, the isoprene precursors were increased in these strains to investigate whether higher titers of amorphadiene could be produced by these mutants. This was achieved by overexpression of MEP pathway enzymes using the pHCMC04G-SDFHCEGA plasmid construct, where seven MEP pathway enzymes Dxs, IspD, IspF, IspH, IspC, IspE, and IspG and downstream farnesyl diphosphate synthase IspA were expressed from a single operon under the control of xylose-inducible promoter $P_{xylA}$ (Figure 3D), since this has been demonstrated to be an efficient approach to increase amorphadiene production by overexpression of all of the MEP pathway genes and *ispA* by providing more precursors.[8] The corresponding strains were 8BSGAF, 8BST399S, 8BSH448A, and 8BSSA. As shown in Figures 3D and S4, none of the three strains with mutations produced higher levels of amorphadiene compared to the wild type.

Ideally, engineering of certain amino acids to significantly improve the catalytic efficiency of rate-limiting enzymes is preferred, since this would facilitate minimizing cell burdens. However, when such mutants are not available, an alternative is to introduce extra copies of this enzyme to release the bottleneck within the synthetic pathway.[20] Therefore, another copy of GFPADS fusion protein was introduced into the genome of BSGAF (mpr::GFPADS), forming strain BSmpr (Figure 3A). Obviously, fermentation results indicated a remarkable increase in the production of amorphadiene by 27% compared with BSGAF (Figures 3E and S4). Further enhancing the MEP pathway in BSmpr (8BSmpr) confirmed the effectiveness of introducing a second copy of GFPADS in *B. subtilis*, as 8BSmpr exhibited 125% amorphadiene production relative to 8BSGAF after 24 h fermentation (Figures 3E and S4).


https://doi.org/10.1021/acs.jafc.1c00498
J. Agric. Food Chem. 2021, 69, 4785−4794

**Engineering of Branch Pathways to Increase Amorphadiene Production.** To provide sufficient FPP for amorphadiene biosynthesis, it is critical to attenuate the branch pathways using FPP as the starting material. For the biosynthesis of $C_{35}$ heptaprenyl diphosphate (HEPP) and $C_{55}$ undecaprenyl pyrophosphate (UDPP) molecules, each FPP requires four and eight molecules of IPP to form HEPP and UDPP, respectively; therefore, they were selected as candidates for branch pathways' engineering (Figure 4A).

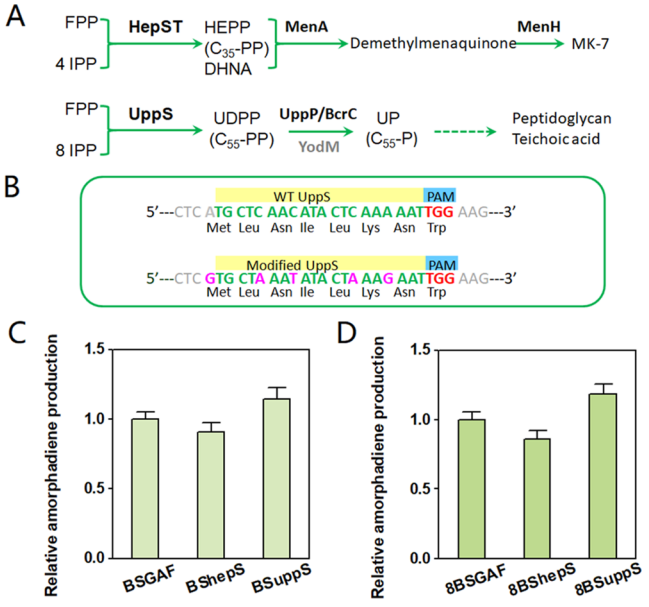


**Figure 4.** Engineering of the branch pathway to improve amorphadiene production in *B. subtilis*. (A) HEPP and UDPP biosynthesis pathway in *B. subtilis*. (B) Start codon and several initial amino acids of UppS have been substituted by a noncanonical start codon (GTG) and corresponding synonymous codons. (C) Relative amorphadiene production in strains with *hepS* knockout and *uppS* mutation after 24 h fermentation. (D) Relative amorphadiene production in strains with MEP pathway overexpression and *hepS* knockout or *uppS* mutation after 24 h fermentation.

Heptaprenyl diphosphate synthase components I and II are encoded by *hepS* and *hepT*, and they exhibited their catalytic activity only when associated together with the cofactor $Mg^{2+}$ and the substrate FPP.[35] Therefore, we knocked out a 110 bp fragment of *hepS* in strain BSGAF to disrupt the function of HepS, thus blocking the synthesis of HEPP (Figure 4A). The resulting strain BShepS was fermented for 24 h, and the production of amorphadiene was measured. Compared with the parent strain BSGAF with entire *hepS* preserved, there was a slight decrease of amorphadiene production (91% relative to BSGAF) and no obvious cell biomass decrease was detected (Figure S5). Undecaprenyl pyrophosphate synthetase (UppS) catalyzes FPP and IPP to form UDPP, and UDPP is an important carrier lipid precursor, which is essential for cell wall synthesis. Hence, to knockdown the expression of UppS in BSGAF strain, the starting codon ATG was substituted by a noncanonical start codon GTG and the second to fourth amino acids were substituted by corresponding synonymous codons, generating BSuppS (Figure 4B). When BSuppS fermentation continued for 24 h, the production of amorphadiene reached 115% relative to the parent strain BSGAF (Figures 4C and S5). In strain 8BSuppS overexpressing the MEP pathway, the amorphadiene production improvement even increased by 19% compared to 8BSGAF (Figures 4C and S5).

**Regulation of the TCA Module to Explore Its Effects on Amorphadiene Production.** Central metabolic pathways could significantly affect terpenoids' production in bacteria through the metabolism of cofactors and energy.[20] Therefore, to explore whether and how TCA metabolism affects amorphadiene production in *B. subtilis*, a strong promoter $P_{hpaII}$ and a weak promoter $P_{liaG}$ were employed to substitute the original promoters of Krebs cycle enzymes of parent strain BSGAF by the CRISPR-Cas9 system (Figure 5C). The generated two sets of strains (BScitZ, BSsucAB, BSsucCD, BSsdhCAB, BScitB, BSfumC contain promoter $P_{hpaII}$; BSlia-citZ, BSlia-sucAB, BSlia-sucCD, BSlia-sdhCAB, BSlia-citB, BSlia-fumC carry promoter $P_{liaG}$) were cultured for 24 h to produce amorphadiene (Figures 5A,B and S6). Results indicated that (i) for strains with a modification of *citB* and *fumC* promoters, no remarkable difference in amorphadiene production was observed compared to BSGAF, regardless of using the strong or weak promoter; (ii) the strong promoter conferred higher amorphadiene titers (89−108%) in strains with engineered promoters of *sucAB*, *sucCD*, and *sdhCAB*, and vice versa with the weak promoter (25−66%); (iii) strains BScitZ and BSlia-citZ resulted in only 30−37% amorphadiene production compared to parent strain BSGAF. This was probably due to the engineered promoters severely affecting the growth of these two strains (Figure S6).

Since the inherent MEP pathway might supply sufficient precursors for relatively low level production of amorphadiene, the potential influence of TCA cycle metabolism might not be fully displayed. Therefore, pHCMC04G-SDFHCEGA was introduced into the strains with strong promoter $P_{hpaII}$, generating 8BScitZ, 8BSsucAB, 8BSsucCD, 8BSsdhCAB, 8BScitB, and 8BSfumC. Investigation results showed that a similar tendency was observed compared to strains without the overexpressed MEP pathway. However, amorphadiene titers produced by strain 8BSsdhCAB were increased to 112% relative to 8BSGAF (Figures 5D and S6), which was a slightly higher improvement (108%) than BSsdhCAB when compared to BSGAF (Figure 5B).

**Combination of Different Modules to Increase Amorphadiene Production.** In this step, we explored whether simultaneous engineering of these modules could produce a synergistic positive effect on amorphadiene production. Hence, strain BSmus was constructed by introducing mpr:GFPADS, UppS mutation, and $P_{hapII}$-sdhCAB to BSGAF. Then, overexpression of MEP pathway genes in BSmus led to strain 8BSmus. Compared to the parental strain 8BSGAF, 8BSmus produced around a 43% higher amount of extracellular amorphadiene, with the production increasing from 81 to 116 mg/L after 48 h fermentation (Figure 6). This significant increase of amorphadiene production of 8BSmus indicated that the extra copy of GFPADS, UppS mutation, and SdhCAB promoter engineering displayed a synergistic effect on improving amorphadiene production. By far, this production is the highest extracellular amorphadiene level that has been reported in *B. subtilis* cultured in medium without optimization in flask-scale fermentation.

## DISCUSSION

Compared to the previously developed genetic engineering tools in *B. subtilis*, the CRISPR-Cas9 system possesses the advantages of easy manipulation, great precision, high editing efficiency, and being a marker-free system. Several CRISPR-based editing


https://doi.org/10.1021/acs.jafc.1c00498
J. Agric. Food Chem. 2021, 69, 4785−4794

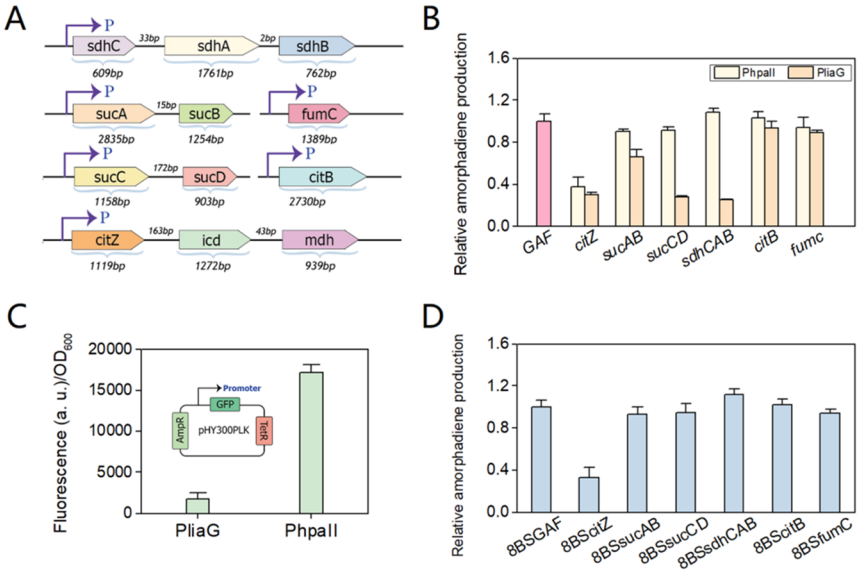


**Figure 5.** Engineering promoters of TCA enzymes to improve amorphadiene production in *B. subtilis*. (A) Operons of TCA enzymes at the genome of *B. subtilis*. (B) Relative amorphadiene production in *B. subtilis* when TCA enzyme promoters were engineered after 24 h fermentation. (C) Scheme of plasmid pHY300PLK used for evaluating promoter strength. Strength of promoters $P_{hpaII}$ and $P_{liaG}$ when using GFP as a reporter gene expressed in *B. subtilis*. PliaG: Promoter $P_{liaG}$; PhpaII: Promoter $P_{hpaII}$. (D) Relative amorphadiene production in strains with TCA enzymes controlled by $P_{hpaII}$ and MEP pathway overexpression after 24 h fermentation.

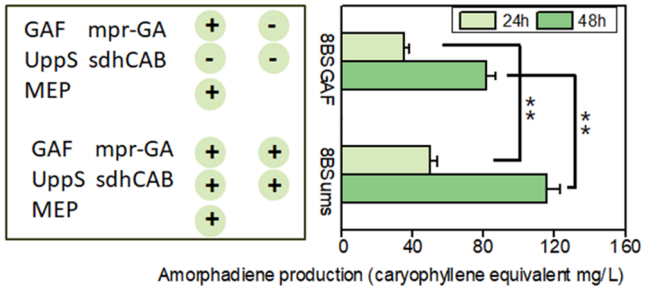


**Figure 6.** Combined strategies to improve amorphadiene production in *B. subtilis*. GAF, fusion protein GFPADS and FppS; mpr: the second copy of fusion protein GFPADS was integrated into the *mpr* gene locus; UppS; UppS mutation; sdhCAB: the promoter of sdhCAB was replaced by strong promoter $P_{hpaII}$; MEP, MEP pathway genes and IspA were overexpressed in plasmid pHCMC04G-SDFHCEGA."−" and "+" represent without and with engineering, respectively. Error bars represent standard deviations of biological triplicates. ** indicates statistically significant differences ($p < 0.05$).

systems have been established in *B. subtilis* to perform gene editing and gene regulation with different efficiencies.[30,32,36,37] The nonhomologous end joining (NHEJ) in *B. subtilis* is too weak to repair the Cas9-induced double-strand break (DSB); thus, editing templates are provided to perform the homology-directed recombination (HDR) and introduce desired mutations. The editing efficiency by donor DNA supplied as PCR products is lower than that by donor DNA provided as part of plasmids, so in this study, the donor DNA was inserted into the plasmid, which simultaneously contains both SpCas9 and the gRNA cassette (Figure 2).[30] Using this system, we were able to not only introduce specific point mutations and knockout genes but also integrate a 2.5 kb GFPADS expression cassette into the genome of *B. subtilis*, which is the largest fragment reported to be integrated into the *B. subtilis* genome by the CRISPR-Cas9 system (Figure 3A).

To introduce only a single amino acid mutation into the genome of *B. subtilis*, the current CRISPR-dCas9-mediated Cs to Ts base editing system could be an option. This system can avoid the dependence on HDR and reduce the fatality rate caused by DSBs, but it requires the participation of cytosine deaminase.[38] After checking the nucleotide sequences of T399 and H448, we found that it is not feasible to introduce the desired mutations by base editing events (Figure 3B). Therefore, to introduce our desired mutations into GFPADS, it is necessary to create the DSBs by SpCas9 near T399 and H448 and introduce editing templates containing inconsistent sequences with N20 nucleotides. Therefore, in addition to introducing T399S or H448A, several nucleotides near the codons T399/H448 and within the N20 sequences are substituted but remain to be synonymous codons that encode unchanged amino acids.

*In vitro*, ADS variants T399S, H448A, and T399S/H448A displayed $K_{cat}$ nearly 2-, 3.5-, and 5-fold higher than that of the wild type, respectively, and the catalytic efficiency ($K_{cat}/K_m$) of mutant H448A increased nearly four times compared with that of the wild type.[33,34] *In vivo*, the expression of T399S, H448A, and T399S/H448A in *E. coli* also increased the production of amorphadiene for nearly 1.7-, 3-, and 4-fold, respectively. However, the promising mutants did not retain these advantages in producing amorphadiene when fused with GFP and expressed in *B. subtilis*; instead, they showed decreased amorphadiene production to a different extent at all growth stages (Figures 2 and S7).

We considered that the high catalytic activities of ADS mutants were observed when enough substrate FPP was provided within the previous *in vitro* assay. Thus, two steps were taken to explore whether sufficient FPP supply could stimulate the mutants presenting higher catalytic activity. The first endeavor of overexpressing MEP pathway genes has shown no improvement in the mutant strains (Figure 3D). Second, the expression levels of GFPADS were reduced by gradually decreasing concentrations of added IPTG at 0.1, 0.01, and 0.001 mM for induction so that the endogenous FPP would be


https://doi.org/10.1021/acs.jafc.1c00498
J. Agric. Food Chem. 2021, 69, 4785−4794

more than enough for the conversion (Figure S8). However, none of the mutants showed higher catalytic power than wild-type GFPADS. Noticeably, the decreased amorphadiene production by GFPADS mutants was not induced by rare codons. That is primarily because there is no strong bias in codon preferences in *B. subtilis*, and only some codons are rarely used including CUA (leucine), AUA (isoleucine), and AGG (arginine), which are not utilized in our mutants (Figure 3B).[39] Second, if the decreased amorphadiene was caused by the low expression level due to rarely used codons, the amorphadiene production produced by the double mutant should be even lower than by the single mutants, which was opposite to our observed results (Figure 3C). Accordingly, the most probable reason to be assumed is that the fusion of the ADS with GFP at the N-terminus influenced the conformation of the enzyme, and the mutations did not improve the catalytic reactions anymore; instead, their introduction even hindered the enzyme activity to some extent. Considering our purpose is to debottleneck the rate-limiting step in the terpene synthase module, further exploration of the underlying mechanism behind the fusion GAFADS was postponed. Thus, an extra copy of the wild-type GFPADS was integrated into the genome of *B. subtilis* to release the bottleneck from this module.

To reduce the consumption of isoprene precursors in the competing pathways, we decided to diminish biosynthesis of HEPP and UDPP, since our previous metabolomics data implied that high concentrations of these two components occurred when the MEP pathway was overexpressed in *B. subtilis*. Therefore, nonessential *hepS* was knocked out and essential *uppS* expression was knocked down using a weak start codon.[40,41] The growth of BShepS was not significantly affected when cultured in a rich fermentation medium, but amorphadiene production decreased to 89% of the parent strains. This might be because HEPP is involved in menaquinone biosynthesis, which plays an important role in electron transport in *B. subtilis*. Considering that disruption of HEPP influenced ATP synthesis, this might contribute to reduced terpenoids' synthesis in less-robust strains.[42]

UppS catalyzes FPP formation with eight consecutive condensation reactions of IPP to form UDPP. Then, UDPP is dephosphorylated by UDPP phosphatases to the monophosphate form UP.[43] This step involves redundant UDPP phosphatases including UppP, BcrC, and the recently predicted YodM (Figure 4A). UDPP and UP are required for the synthesis of both peptidoglycan and wall teichoic acids, the predominant components of the *B. subtilis* cell envelope. To repress the expression level of UppS, we used GUG to replace the classical start codon AUG and the second leucine was also substituted by the rare codon CUA (Figure 4B).[39] It was assumed that decreasing UppS expression would lead to less FPP and IPP consumption and the UDPP and UP recycling process would be compensated for and replenished by the increased activities of UDPP phosphatases.[44,45] Thus, the cell wall synthesis and growth of *B. subtilis* was not significantly affected, but the amorphadiene production increased by 15−19% (Figure 4C,D).

As the fundamental hub of the metabolic network, the TCA cycle provides the cell with energy, cellular building blocks, and cofactors, affecting numerous connected metabolic pathways directly or indirectly.[41] In this step, a critical investigation was conducted to screen which steps of the TCA cycle influence terpenoid production. A previous study showed that supplementing the growth medium with extra pyruvate could sharply increase amorphadiene production.[8] This implied that repressing the TCA cycle to consume less pyruvate could be a potential strategy for higher amorphadiene production. However, in another case, enhancing some TCA cycle enzymes to guarantee a sufficient supply of cofactors also remarkably increased terpenoid production.[20] Those results inspired us to explore the effects of both upregulation and downregulation of the TCA cycle on amorphadiene production.

Many associated enzymes from the TCA module are organized as large operons, which makes it difficult to amplify them for further overexpression (Figure 5A). Modulating their expression levels at the genomic level using promoters with different strengths provides a good solution.[20] To clearly distinguish which steps have the most influence, we selected both strong and weak promoters to regulate their expression (Figure 5C).[46,47] Results displayed that for the first time we were able to distinguish three different types of influences, namely, engineering promoters of TCA enzymes could produce (i) a negative influence on amorphadiene production, (ii) a non-obvious influence on amorphadiene production, and (iii) different influences on amorphadiene production according to the promoter strength (Figure 5B). In addition, engineering operon *citZ-icd-mdh* resulted in a severe decrease in amorphadiene production. In bacteria, an imbalanced ratio of reducing forces (NAD+/NADH, NADP+/NADPH) has been shown to enormously decrease the formation of the desired products.[48] It was assumed that expression levels of Mdh and Icd after engineering did not meet this balance since this operon is involved in the metabolism of NADH and NADPH simultaneously (Figure 1).[49] Interestingly, levels of amorphadiene production were much higher when SucAB, SucCD, and SdhCAB were controlled by the strong promoter $P_{hpaII}$ than by the weak promoter $P_{liaG}$. These results provide us a promising strategy for further improvement of amorphadiene production, such as employing promoters that are even stronger than $P_{hpaII}$ to those enzymes. Though all of the three operons are related to the metabolism of cofactors, the mechanism behind them is still unknown. Conclusively, the promoter engineering step gave us an overview of how the TCA cycle could impact amorphadiene production and pointed to several prospective candidates for further engineering. Undoubtedly, deep insights into many aspects still need to be explored. First, influences from the combined upregulation and downregulation of TCA enzymes require additional clarification. Second, effects from other central metabolic pathways including the pentose phosphate pathway and glycolysis are also critical to be evaluated. Third, the underlying mechanisms remain to be elucidated. Finally, combining all of the promising engineering modules in one strain 8BSmus showed around 43% higher extracellular amorphadiene compared to the parent strain 8BSGAF, with the production reaching from 81 to 116 mg/L after 48 h fermentation. Of note, higher productions of amorphadiene have been achieved by some other well-studied microorganisms after sophisticated and comprehensive engineering, including *E. coli*, *Saccharomyces cerevisiae*, and nonconventional yeast *Yarrowia lipolytica*, with the productions of amorphadiene reaching 30 g/L in fed-batch fermentation for 80 h, 41 g/L in fed-batch fermentation for 116 h, and 171.5 mg/L in shake flask for 144 h, respectively.[50−52] Though the yeast strains have the disadvantage of relatively long fermentation time compared with *B. subtilis* and the *E. coli* strains face the challenge of producing endotoxins, these studies still provide useful strategies that could be explored in *B. subtilis* to further improve amorphadiene productions. These include introducing the heterologous


https://doi.org/10.1021/acs.jafc.1c00498
J. Agric. Food Chem. 2021, 69, 4785−4794

mevalonate (MVA) pathway to *B. subtilis*, balancing the expression levels of the MVA pathway enzymes at transcription and translation levels, engineering terpene synthases by random mutations, and optimizing fermentation medium and processes in bioreactions and fermenters.

## ■ ASSOCIATED CONTENT

### Supporting Information

The Supporting Information is available free of charge at https://pubs.acs.org/doi/10.1021/acs.jafc.1c00498.

Plasmids used in this study (Table S1); strains used in this study (Table S2); prolonged incubation procedure in *B. subtilis* transformation (Figure S1); primer design to screen promising positive colonies of CRISPR-cas9-engineered strains (Figure S2); amorphadiene production levels and fluorescence of fusion protein GFPADS at different temperatures (Figure S3); amorphadiene production levels of *B. subtilis* strains with ADS mutations and MEP pathway overexpression (Figure S4); amorphadiene production levels and biomass of *B. subtilis* strains with engineered branch pathways (Figure S5); amorphadiene production levels and biomass of *B. subtilis* strains with engineered promoters of TCA enzymes (Figure S6); amorphadiene production levels at different time points (Figure S7); amorphadiene production when induced with different IPTG concentrations (Figure S8) (PDF)

## ■ AUTHOR INFORMATION


### Corresponding Author

**Wim J. Quax** − *Department of Chemical and Pharmaceutical Biology, Groningen Research Institute of Pharmacy, University of Groningen, 9713 AV Groningen, The Netherlands;* orcid.org/0000-0002-5162-9947; Phone: +31 (0) 50 363 2558; Email: w.j.quax@rug.nl; Fax: +31 (0) 50 363 3000

### Authors

**Yafeng Song** − *Department of Chemical and Pharmaceutical Biology, Groningen Research Institute of Pharmacy, University of Groningen, 9713 AV Groningen, The Netherlands*

**Siqi He** − *Department of Chemical and Pharmaceutical Biology, Groningen Research Institute of Pharmacy, University of Groningen, 9713 AV Groningen, The Netherlands*

**Ingy I. Abdallah** − *Department of Chemical and Pharmaceutical Biology, Groningen Research Institute of Pharmacy, University of Groningen, 9713 AV Groningen, The Netherlands; Department of Pharmacognosy, Faculty of Pharmacy, Alexandria University, 21521 Alexandria, Egypt*

**Anita Jopkiewicz** − *Department of Chemical and Pharmaceutical Biology, Groningen Research Institute of Pharmacy, University of Groningen, 9713 AV Groningen, The Netherlands*

**Rita Setroikromo** − *Department of Chemical and Pharmaceutical Biology, Groningen Research Institute of Pharmacy, University of Groningen, 9713 AV Groningen, The Netherlands*

**Ronald van Merkerk** − *Department of Chemical and Pharmaceutical Biology, Groningen Research Institute of Pharmacy, University of Groningen, 9713 AV Groningen, The Netherlands*

**Pieter G. Tepper** − *Department of Chemical and Pharmaceutical Biology, Groningen Research Institute of Pharmacy, University of Groningen, 9713 AV Groningen, The Netherlands*

Complete contact information is available at: https://pubs.acs.org/10.1021/acs.jafc.1c00498


### Notes

The authors declare no competing financial interest.

## ■ ACKNOWLEDGMENTS

Y.S. and S.H. acknowledge funding from the China Scholarship Council.

## ■ ABBREVIATIONS USED

ADS, amorphadiene synthase; CRISPR-Cas9, clustered regularly interspaced short palindromic repeat-Cas9; IPP, isopentenyl pyrophosphate; DMAPP, dimethylallyl pyrophosphate; GPP, geranyl pyrophosphate; FPP, farnesyl pyrophosphate; GGPP, geranylgeranyl pyrophosphate; MEP, 2-*C*-methyl-D-erythritol 4-phosphate; HMBPP, 1-hydroxy-2-methyl-2-butenyl 4-pyrophosphate; GFP, green fluorescent protein; HEPP, heptaprenyl diphosphate; UDPP, undecaprenyl pyrophosphate; TCA, tricarboxylic acid

## ■ REFERENCES


(1) Bohlmann, J.; Keeling, C. I. Terpenoid biomaterials. *Plant J.* **2008**, *54*, 656−669.

(2) Tholl, D. Biosynthesis and biological functions of terpenoids in plants. *Adv. Biochem. Eng./Biotechnol.* **2015**, *148*, 63−106.

(3) Nagegowda, D. A.; Gupta, P. Advances in biosynthesis, regulation, and metabolic engineering of plant specialized terpenoids. *Plant Sci.* **2020**, *294*, No. 110457.

(4) Martin, V. J.; Pitera, D. J.; Withers, S. T.; Newman, J. D.; Keasling, J. D. Engineering a mevalonate pathway in *Escherichia coli* for production of terpenoids. *Nat. Biotechnol.* **2003**, *21*, 796−802.

(5) Paddon, C. J.; Westfall, P. J.; Pitera, D. J.; Benjamin, K.; Fisher, K.; McPhee, D.; Leavell, M. D.; Tai, A.; Main, A.; Eng, D.; Polichuk, D. R.; Teoh, K. H.; Reed, D. W.; Treynor, T.; Lenihan, J.; Fleck, M.; Bajad, S.; Dang, G.; Dengrove, D.; Diola, D.; Dorin, G.; Ellens, K. W.; Fickes, S.; Galazzo, J.; Gaucher, S. P.; Geistlinger, T.; Henry, R.; Hepp, M.; Horning, T.; Iqbal, T.; Jiang, H.; Kizer, L.; Lieu, B.; Melis, D.; Moss, N.; Regentin, R.; Secrest, S.; Tsuruta, H.; Vazquez, R.; Westblade, L. F.; Xu, L.; Yu, M.; Zhang, Y.; Zhao, L.; Lievense, J.; Covello, P. S.; Keasling, J. D.; Reiling, K. K.; Renninger, N. S.; Newman, J. D. High-level semi-synthetic production of the potent antimalarial artemisinin. *Nature* **2013**, *496*, 528−532.

(6) Ajikumar, P. K.; Xiao, W. H.; Tyo, K. E.; Wang, Y.; Simeon, F.; Leonard, E.; Mucha, O.; Phon, T. H.; Pfeifer, B.; Stephanopoulos, G. Isoprenoid pathway optimization for Taxol precursor overproduction in *Escherichia coli*. *Science* **2010**, *330*, 70−74.

(7) Zhang, Y.; Nielsen, J.; Liu, Z. Engineering yeast metabolism for production of terpenoids for use as perfume ingredients, pharmaceuticals and biofuels. *FEMS Yeast Res.* **2017**, *17*, No. fox080.

(8) Pramastya, H.; Xue, D.; Abdallah, I. I.; Setroikromo, R.; Quax, W. J. High level production of amorphadiene using *Bacillus subtilis* as an optimized terpenoid cell factory. *New Biotechnol.* **2021**, *60*, 159−167.

(9) Pramastya, H.; Song, Y.; Elfahmi, E. Y.; Sukrasno, S.; Quax, W. J. Positioning *Bacillus subtilis* as terpenoid cell factory. *J. Appl. Microbiol.* **2020**, DOI: 10.1111/jam.14904.

(10) Zhou, K.; Zou, R.; Zhang, C.; Stephanopoulos, G.; Too, H. P. Optimization of amorphadiene synthesis in *Bacillus subtilis* via transcriptional, translational, and media modulation. *Biotechnol. Bioeng.* **2013**, *110*, 2556−2561.

(11) Gomaa, L.; Loscar, M. E.; Zein, H. S.; Abdel-Ghaffar, N.; Abdelhadi, A. A.; Abdelaal, A. S.; Abdallah, N. A. Boosting isoprene production via heterologous expression of the Kudzu isoprene synthase

gene (kIspS) into *Bacillus spp*. cell factory. *AMB Express* **2017**, *7*, No. 161.
(12) Abdallah, I. I.; Pramastya, H.; van Merkerk, R.; Sukrasno; Quax, W. J. Metabolic Engineering of *Bacillus subtilis* Toward Taxadiene Biosynthesis as the First Committed Step for Taxol Production. *Front. Microbiol.* **2019**, *10*, No. 218.
(13) Yoshida, K.; Ueda, S.; Maeda, I. Carotenoid production in *Bacillus subtilis* achieved by metabolic engineering. *Biotechnol. Lett.* **2009**, *31*, 1789−1793.
(14) Xue, D.; Abdallah, I. I.; de Haan, I. E.; Sibbald, M. J.; Quax, W. J. Enhanced C30 carotenoid production in *Bacillus subtilis* by systematic overexpression of MEP pathway genes. *Appl. Microbiol. Biotechnol.* **2015**, *99*, 5907−5915.
(15) Abdallah, I. I.; Xue, D.; Pramastya, H.; van Merkerk, R.; Setroikromo, R.; Quax, W. J. A regulated synthetic operon facilitates stable overexpression of multigene terpenoid pathway in *Bacillus subtilis*. *J. Ind. Microbiol. Biotechnol.* **2020**, *47*, 243−249.
(16) Song, Y.; Guan, Z.; van Merkerk, R.; Pramastya, H.; Abdallah, I. I.; Setroikromo, R.; Quax, W. J. Production of Squalene in *Bacillus subtilis* by Squalene Synthase Screening and Metabolic Engineering. *J. Agric. Food Chem.* **2020**, *68*, 4447−4455.
(17) Yang, S.; Cao, Y.; Sun, L.; Li, C.; Lin, X.; Cai, Z.; Zhang, G.; Song, H. Modular Pathway Engineering of *Bacillus subtilis* To Promote De Novo Biosynthesis of Menaquinone-7. *ACS Synth. Biol.* **2019**, *8*, 70−81.
(18) Ma, Y.; McClure, D. D.; Somerville, M. V.; Proschogo, N. W.; Dehghani, F.; Kavanagh, J. M.; Coleman, N. V. Metabolic Engineering of the MEP Pathway in *Bacillus subtilis* for Increased Biosynthesis of Menaquinone-7. *ACS Synth. Biol.* **2019**, *8*, 1620−1630.
(19) Cui, S.; Lv, X.; Wu, Y.; Li, J.; Du, G.; Ledesma-Amaro, R.; Liu, L. Engineering a Bifunctional Phr60-Rap60-Spo0A Quorum-Sensing Molecular Switch for Dynamic Fine-Tuning of Menaquinone-7 Synthesis in *Bacillus subtilis*. *ACS Synth. Biol.* **2019**, *8*, 1826−1837.
(20) Zhao, J.; Li, Q.; Sun, T.; Zhu, X.; Xu, H.; Tang, J.; Zhang, X.; Ma, Y. Engineering central metabolic modules of *Escherichia coli* for improving beta-carotene production. *Metab. Eng.* **2013**, *17*, 42−50.
(21) Cui, S.; Xia, H.; Chen, T.; Gu, Y.; Lv, X.; Liu, Y.; Li, J.; Du, G.; Liu, L. Cell Membrane and Electron Transfer Engineering for Improved Synthesis of Menaquinone-7 in *Bacillus subtilis*. *iScience* **2020**, *23*, No. 100918.
(22) Hess, B. M.; Xue, J.; Markillie, L. M.; Taylor, R. C.; Wiley, H. S.; Ahring, B. K.; Linggi, B. Coregulation of Terpenoid Pathway Genes and Prediction of Isoprene Production in *Bacillus subtilis* Using Transcriptomics. *PLoS One* **2013**, *8*, No. e66104.
(23) Meyer, H.; Weidmann, H.; Mader, U.; Hecker, M.; Volker, U.; Lalk, M. A time resolved metabolomics study: the influence of different carbon sources during growth and starvation of *Bacillus subtilis*. *Mol. BioSyst.* **2014**, *10*, 1812−1823.
(24) Ravikumar, V.; Nalpas, N. C.; Anselm, V.; Krug, K.; Lenuzzi, M.; Sestak, M. S.; Domazet-Loso, T.; Mijakovic, I.; Macek, B. In-depth analysis of *Bacillus subtilis* proteome identifies new ORFs and traces the evolutionary history of modified proteins. *Sci. Rep.* **2018**, *8*, No. 17246.
(25) Koo, B. M.; Kritikos, G.; Farelli, J. D.; Todor, H.; Tong, K.; Kimsey, H.; Wapinski, I.; Galardini, M.; Cabal, A.; Peters, J. M.; Hachmann, A. B.; Rudner, D. Z.; Allen, K. N.; Typas, A.; Gross, C. A. Construction and Analysis of Two Genome-Scale Deletion Libraries for *Bacillus subtilis*. *Cell Syst.* **2017**, *4*, 291−305 e7.
(26) Nicolas, P.; Mader, U.; Dervyn, E.; Rochat, T.; Leduc, A.; Pigeonneau, N.; Bidnenko, E.; Marchadier, E.; Hoebeke, M.; Aymerich, S.; Becher, D.; Bisicchia, P.; Botella, E.; Delumeau, O.; Doherty, G.; Denham, E. L.; Fogg, M. J.; Fromion, V.; Goelzer, A.; Hansen, A.; Härtig, E.; Harwood, C. R.; Homuth, G.; Jarmer, H.; Jules, M.; Klipp, E.; Chat, L. L.; Lecointe, F.; Lewis, P.; Liebermeister, W.; March, A.; Mars, R. A. T.; Nannapaneni, P.; Noone, D.; Pohl, S.; Rinn, B.; Rügheimer, F.; Sappa, P. K.; Samson, F.; Schaffer, M.; Schwikowski, B.; Steil; Stülke, J.; Wiegert, T.; Devine, K. M.; Wilkinson, A. J.; van Dijl, J. M.; Hecker, M.; Völker, U.; Bessières, P.; Noirot, P. Condition-dependent transcriptome reveals high-level regulatory architecture in *Bacillus subtilis*. *Science* **2012**, *335*, 1103−1106.
(27) Dong, H.; Zhang, D. Current development in genetic engineering strategies of *Bacillus* species. *Microb. Cell Fact.* **2014**, *13*, No. 63.
(28) Gupta, D.; Bhattacharjee, O.; Mandal, D.; Sen, M. K.; Dey, D.; Dasgupta, A.; Kazi, T. A.; Gupta, R.; Sinharoy, S.; Acharya, K.; Chattopadhyay, V.; Ravichandiran, D.; Roy, S.; Ghosh, D. CRISPR-Cas9 system: A new-fangled dawn in gene editing. *Life Sci.* **2019**, *232*, No. 116636.
(29) You, C.; Zhang, X. Z.; Zhang, Y. H. Simple cloning via direct transformation of PCR product (DNA Multimer) to *Escherichia coli* and *Bacillus subtilis*. *Appl. Environ. Microbiol.* **2012**, *78*, 1593−1595.
(30) Westbrook, A. W.; Moo-Young, M.; Chou, C. P. Development of a CRISPR-Cas9 Tool Kit for Comprehensive Engineering of *Bacillus subtilis*. *Appl. Environ. Microbiol.* **2016**, *82*, 4876−4895.
(31) Kunst, F.; Rapoport, G. Salt stress is an environmental signal affecting degradative enzyme synthesis in *Bacillus subtilis*. *J. Bacteriol.* **1995**, *177*, 2403−2407.
(32) Altenbuchner, J. Editing of the *Bacillus subtilis* Genome by the CRISPR-Cas9 System. *Appl. Environ. Microbiol.* **2016**, *82*, 5421−5427.
(33) Li, J. X.; Fang, X.; Zhao, Q.; Ruan, J. X.; Yang, C. Q.; Wang, L. J.; Miller, D. J.; Faraldos, J. A.; Allemann, R. K.; Chen, X. Y.; Zhang, P. Rational engineering of plasticity residues of sesquiterpene synthases from *Artemisia annua*: product specificity and catalytic efficiency. *Biochem. J.* **2013**, *451*, 417−426.
(34) Abdallah, I. I.; van Merkerk, R.; Klumpenaar, E.; Quax, W. J. Catalysis of amorpha-4,11-diene synthase unraveled and improved by mutability landscape guided engineering. *Sci. Rep.* **2018**, *8*, No. 9961.
(35) Suzuki, T.; Zhang, Y. W.; Koyama, T.; Sasaki, D. Y.; Kurihara, K. Direct observation of substrate−enzyme complexation by surface forces measurement. *J. Am. Chem. Soc.* **2006**, *128*, 15209−15214.
(36) Price, M. A.; Cruz, R.; Baxter, S.; Escalettes, F.; Rosser, S. J. CRISPR-Cas9 In Situ engineering of subtilisin E in *Bacillus subtilis*. *PLoS One* **2019**, *14*, No. e0210121.
(37) So, Y.; Park, S. Y.; Park, E. H.; Park, S. H.; Kim, E. J.; Pan, J. G.; Choi, S. K. A Highly Efficient CRISPR-Cas9-Mediated Large Genomic Deletion in *Bacillus subtilis*. *Front. Microbiol.* **2017**, *8*, No. 1167.
(38) Yu, S.; Price, M. A.; Wang, Y.; Liu, Y.; Guo, Y.; Ni, X.; Rosser, S. J.; Bi, C.; Wang, M. CRISPR-dCas9 Mediated Cytosine Deaminase Base Editing in *Bacillus subtilis*. *ACS Synth. Biol.* **2020**, *9*, 1781−1789.
(39) Moszer, I.; Rocha, E. P.; Danchin, A. Codon usage and lateral gene transfer in *Bacillus subtilis*. *Curr. Opin. Microbiol.* **1999**, *2*, 524−528.
(40) Wu, Z.; Zhao, D.; Li, S.; Wang, J.; Bi, C.; Zhang, X. Combinatorial modulation of initial codons for improved zeaxanthin synthetic pathway efficiency in *Escherichia coli*. *MicrobiologyOpen* **2019**, *8*, No. e930.
(41) Gu, Y.; Deng, J.; Liu, Y.; Li, J.; Shin, H. D.; Du, G.; Chen, J.; Liu, L. Rewiring the Glucose Transportation and Central Metabolic Pathways for Overproduction of *N*-Acetylglucosamine in *Bacillus subtilis*. *Biotechnol. J.* **2017**, *12*, No. 1700020.
(42) Pelchovich, G.; Omer-Bendori, S.; Gophna, U. Menaquinone and iron are essential for complex colony development in *Bacillus subtilis*. *PLoS One* **2013**, *8*, No. e79488.
(43) Jorgenson, M. A.; Kannan, S.; Laubacher, M. E.; Young, K. D. Dead-end intermediates in the enterobacterial common antigen pathway induce morphological defects in *Escherichia coli* by competing for undecaprenyl phosphate. *Mol. Microbiol.* **2016**, *100*, 1−14.
(44) Zhao, H.; Sun, Y.; Peters, J. M.; Gross, C. A.; Garner, E. C.; Helmann, J. D. Depletion of Undecaprenyl Pyrophosphate Phosphatases Disrupts Cell Envelope Biogenesis in *Bacillus subtilis*. *J. Bacteriol.* **2016**, *198*, 2925−2935.
(45) Inaoka, T.; Ochi, K. Undecaprenyl pyrophosphate involvement in susceptibility of *Bacillus subtilis* to rare earth elements. *J. Bacteriol.* **2012**, *194*, 5632−5637.
(46) Radeck, J.; Kraft, K.; Bartels, J.; Cikovic, T.; Durr, F.; Emenegger, J.; Kelterborn, S.; Sauer, C.; Fritz, G.; Gebhard, S.; Mascher, T. The Bacillus BioBrick Box: generation and evaluation of essential genetic building blocks for standardized work with *Bacillus subtilis*. *J. Biol. Eng.* **2013**, *7*, No. 29.


https://doi.org/10.1021/acs.jafc.1c00498
J. Agric. Food Chem. 2021, 69, 4785−4794

(47) Zhang, M.; Shi, M.; Zhou, Z.; Yang, S.; Yuan, Z.; Ye, Q. Production of Alcaligenes faecalis penicillin G acylase in *Bacillus subtilis* WB600 (pMA5) fed with partially hydrolyzed starch. *Enzyme Microb. Technol.* **2006**, *39*, 555−560.
(48) Qi, H.; Li, S.; Zhao, S.; Huang, D.; Xia, M.; Wen, J. Model-driven redox pathway manipulation for improved isobutanol production in *Bacillus subtilis* complemented with experimental validation and metabolic profiling analysis. *PLoS One* **2014**, *9*, No. e93815.
(49) Bartholomae, M.; Meyer, F. M.; Commichau, F. M.; Burkovski, A.; Hillen, W.; Seidel, G. Complex formation between malate dehydrogenase and isocitrate dehydrogenase from *Bacillus subtilis* is regulated by tricarboxylic acid cycle metabolites. *FEBS J.* **2014**, *281*, 1132−1143.
(50) Westfall, P. J.; Pitera, D. J.; Lenihan, J. R.; Eng, D.; Woolard, F. X.; Regentin, R.; Horning, T.; Tsuruta, H.; Melis, D. J.; Owens, A.; Fickes, S.; Diola, D.; Benjamin, K. R.; Keasling, J. D.; Leavell, M. D.; McPhee, D. J.; Renninger, N. S.; Newman, J. D.; Paddon, C. J. Production of amorphadiene in yeast, and its conversion to dihydroartemisinic acid, precursor to the antimalarial agent artemisinin. *Proc. Natl. Acad. Sci. U.S.A.* **2012**, *109*, E111−E118.
(51) Shukal, S.; Chen, X.; Zhang, C. Systematic engineering for high-yield production of viridiflorol and amorphadiene in auxotrophic *Escherichia coli*. *Metab. Eng.* **2019**, *55*, 170−178.
(52) Marsafari, M.; Xu, P. Debottlenecking mevalonate pathway for antimalarial drug precursor amorphadiene biosynthesis in *Yarrowia lipolytica*. *Metab. Eng. Commun.* **2020**, *10*, No. e00121.



https://doi.org/10.1021/acs.jafc.1c00498
*J. Agric. Food Chem.* 2021, 69, 4785−4794